Hole-burning spectra of tropolone-(CO2)n (n=1,2) van der Waals complexes and density functional study

ARTICLE *in* CHEMICAL PHYSICS · AUGUST 2001

Impact Factor: 1.65 · DOI: 10.1016/S0301-0104(01)00399-8

5 AUTHORS, INCLUDING:

Norifumi Yamamoto
Chiba Institute of Technology
27 PUBLICATIONS **281** CITATIONS

ELSEVIER

Chemical Physics 270 (2001) 333–343

Chemical Physics

www.elsevier.com/locate/chemphys

Hole-burning spectra of tropolone–$(CO_2)_n$ ($n = 1, 2$) van der Waals complexes and density functional study

Kunihiko Iwahashi, Norifumi Yamamoto, Tetsuro Fukuchi, Jyunya Furusawa, Hiroshi Sekiya *

Department of Chemistry, Faculty of Sciences, Graduate School of Molecular Chemistry, Kyushu University, 6-10-1 Hakozaki, Higashi-ku, Fukuoka 812-8581, Japan

Received 12 March 2001

Abstract

The hole-burning, fluorescence excitation, and dispersed fluorescence spectra of jet-cooled tropolone (TRN)–$(CO_2)_n$ ($n = 1, 2$) complexes are measured to investigate the structures of the complexes and the effects of intermolecular interaction on proton tunneling in TRN. The electronic transitions of TRN–$(CO_2)_n$ ($n = 1, 2$) are well separated in the hole-burning spectrum. Only the transitions of one species have been identified for the 1:1 and 1:2 complexes. Structures of TRN–$(CO_2)_n$ ($n = 1, 2$) are optimized by the density functional theory calculations at the B3LYP/cc-pVDZ level. Three local minima have been obtained for both the 1:1 and 1:2 complexes. In the 1:1 complex CO_2 is bonded in the molecular plane close to a solvation site, C=O (Isomer I), C=O···H–O (Isomer II), or C=O (Isomer III). These complexes are stabilized mainly by the dipole–quadrupole interaction, and the binding energies for these complexes are estimated to be much smaller than those for the hydrogen-bonded complexes. Isomers I and II are plausible candidates for the observed species. The calculations imply that asymmetry of the double-minimum potential well along the tunneling coordinates of TRN–$(CO_2)_1$ is large enough to quench proton tunneling. This prediction is consistent with the nonobservation of the tunneling splittings even for the excitation of the tunneling promoting mode $\nu_{13}(a_1)$ or $\nu_{14}(a_1)$ of TRN.

1. Introduction

Tropolone (TRN) is one of the most extensively studied polyatomic molecules which exhibit intramolecular proton tunneling. Spectroscopic studies of TRN in the isolated state together with theoretical studies unambiguously showed multidimensional nature of proton tunneling in TRN [1–21]. We note that the tunneling splittings measured in a rare gas matrix [22] are significantly different from those in a supersonic jet, and the tunneling splitting drastically changes in a mixed crystal [23]. These observations imply that the intermolecular interactions influence the probability of proton tunneling in the condensed phase. In order to understand proton tunneling in the condensed phase it is important to investigate molecular systems where intermolecular coordinates are well defined. Thus we have studied the effects of intermolecular interactions on proton tunneling microscopically by measuring the electronic spectra of various complexes of TRN with solvent

* Corresponding author. Tel.: +81-92-642-2574; fax: +81-92-642-2607.

E-mail address: hsekiscc@mbox.nc.kyushu-u.ac.jp (H. Sekiya).

0301-0104/01/$ - see front matter
PII: S0301-0104(01)00399-8

atom or molecule cooled in a supersonic jet. Such complexes can be regarded as a model system for the investigation of multidimensional proton tunneling, in which the intermolecular coordinates are added to the intramolecular coordinates.

The TRN–M complexes, where M is the solvent atom or molecule, studied so far are classified into two types. One is the hydrogen-bonded complexes in which polar molecules such as H_2O [24–27], CH_3OH [26], and CH_3COCH_3 [28] are bonded to the OH and/or C=O group. In these complexes the tunneling splittings are not observed due to significant change in the shape of the double-minimum potential well along the tunneling coordinate. The other type is van der Waals (vdW) complexes. In the TRN–M (M = Rg, CH_4, N_2, CO, etc.) complexes, M binds above the molecular plane of the seven-membered ring [29–35]. The magnitude of the tunneling splitting of the zero-point level in the S_1 state significantly depends on the polarizability and also the number of solvent molecules. The attachment of the Rg (Ar, Kr, Xe) atom does not significantly change the tunneling splitting [29]. But the binding of a molecule such as N_2, or CO with an anisotropic polarizability to TRN either remarkably decreases the tunneling splitting or completely quenches the tunneling splitting [30–35]. We have explained the decreases in the tunneling splittings by coupling of the intermolecular vibrations with the intramolecular vibrations of TRN, which substantially increases the tunneling potential energy barrier [33].

Recently, MacKenzie et al. observed another type of TRN complex [36,37]. In the fluorescence excitation spectrum of TRN–CO_2, the electronic origin bands of the 1:1 and 1:2 complexes were 99.0 and 126.5 cm^{-1} blue-shifted from that of TRN [36,37]. It was suggested that the CO_2 molecule is located in the molecular plane of TRN, although the other nonpolar solvent molecules lie above the seven-membered ring of TRN. Numerous studies have been carried out on the vdW complexes in which the solvent molecule or atom is bonded on the molecular plane of the aromatic ring. However, little is known about the vdW complexes of aromatic or pseudoaromatic molecules having planar structure. More detailed study on the TRN–CO_2 complex may provide insights into weak intermolecular interactions between the pseudoaromatic molecule and nonpolar solvent molecules and its effects on proton tunneling in TRN.

In the previous study on TRN–$(CO_2)_n$ ($n = 1, 2$) [36,37], only the fluorescence excitation spectrum was measured, and the vibrational frequencies in the higher frequency region ($\nu \geqslant 0$–$0 + 200$ cm^{-1}) as well as those in the S_0 state have not been determined. The structure of the observed species was predicted by ab initio calculations at the RHF/6-31G* level [37], however, the calculations may be insufficient to estimate the binding energies for the TRN–$(CO_2)_n$ ($n = 1, 2$) complexes. Thus we have re-investigated the electronic spectrum of TRN–$(CO_2)_n$ ($n = 1, 2$) in a supersonic jet expansion by measuring the dispersed fluorescence and hole-burning spectra as well as the fluorescence excitation spectrum. The hole-burning spectroscopy is useful to separate the vibronic bands of different size clusters. The measurement of the vibrational frequencies of the intermolecular modes in the electronic ground state is very helpful to determine the structure of the complex, because the calculations for the ground state are more easy and reliable than those for the excited electronic state. We have used the density functional theory (DFT) at the B3LYP/cc-pVDZ level with a GAUSSIAN 98 program package [38] to obtain stable structures and intermolecular vibrational frequencies. Three isomers have been obtained for both the 1:1 and 1:2 complexes. The effects of the intermolecular interactions on the structure of the complex and the intramolecular proton tunneling have been discussed.

2. Experimental

The experimental apparatus used was essentially the same as that used previously [33]. The vacuum chamber was evacuated by a 10 in. diffusion pump backed by a 1200 l/min oil rotary pump. The nozzle housing was heated to 100°C with a coiled heater to obtain sufficient vapor pressure for the measurement of the spectrum. The CO_2 gas was diluted with the helium carrier gas in a stainless steel vessel, which was mixed with

vaporized TRN and expanded into the vacuum chamber with a pulsed nozzle (general valve $D = 0.5$ mm). The backing pressure of He (P_0) was 2–5 atm, and the partial pressure of CO_2 was estimated to be 1–10 Torr. The S_1–S_0 ($\pi\pi^*$) transitions of the complexes produced in a free jet was probed with a XeCl excimer laser pumped dye laser (Lumonics HE700 and HD300). Total fluorescence was detected with a photomultiplier (Hamamatsu 1P28A), while scanning the wavelength of the dye laser to measure the excitation spectrum. The photocurrent signal was averaged with a digital storagescope (LeCroy 9400). The frequency doubled output of the idler light of a MOPO system (Spectra Physics) was used for the probe laser, while the output of the dye laser system (Lumonics HE700 and HD300) was employed for the pump laser to obtain the hole-burning spectrum. The two beams were irradiated on the molecular beam from the opposite directions. The beam of the probe laser was unfocused, while that of the pump laser was mildly focused. A typical delay time between the pump and probe lasers was 300 ns. The fluorescence-dip signal was detected with a photomultiplier and averaged with a storagescope while scanning the wavelength of the pump laser.

3. Results and discussion

3.1. Fluorescence excitation and hole-burning spectra

Fig. 1c shows the laser-induced fluorescence (LIF) excitation spectrum of TRN–$(CO_2)_n$. Two prominent bands are observed at 27 116 and 27 143 cm^{-1}. The frequencies of these bands are 98 and 125 cm^{-1} blue-shifted with respect to the electronic origin band of the monomer, respectively. Many vibronic transitions are detected in the blue region of the origin band of TRN. To identify these transitions we have measured the hole-burning spectra by probing the bands at 98 and 125 cm^{-1}, which are shown in Fig. 1b and c, respectively. A comparison of the hole-burning spectra with the LIF spectrum indicates that two prominent transition systems are involved in the LIF spectrum of TRN–CO_2. The vibronic pattern in the hole-burning spectrum (Fig. 1a) is similar to that of the monomer, whereas the pattern in Fig. 1b is substantially different. The intensity of the bands in Fig. 1b increased with the concentration of CO_2. On the basis of these results we ascribed the spectra shown in Fig. 1a and b to the 1:1 and 1:2 complexes of TRN with CO_2, respectively. This assignment is consistent with the previous one [36,37]. Only the transitions of one species have been identified both for the 1:1 and 1:2 complexes.

In the hole-burning spectrum of TRN–CO_2 the transitions involving the vibrational modes of TRN, $\nu_{25}(a_2)$, $\nu_{26}(a_2)$, $\nu_{13}(a_1)$, and $\nu_{14}(a_1)$ [5,8], are observed in addition to the intermolecular vibrations. It is known that ν_{25} and ν_{26} are tunneling suppressing modes, whereas ν_{13} and ν_{14} are tunneling promoting modes of TRN, respectively. The excitation of $\nu_{25}(a_2)$ or $\nu_{26}(a_2)$ mode decreases the magnitude of tunneling splitting as compared with that of the zero-point level, whereas the excitation of the $\nu_{13}(a_1)$ or $\nu_{14}(a_1)$ increases the magnitude of tunneling splitting [5,8]. The frequencies of vibronic bands and their assignments are listed in Table 1. An intermolecular vibration is observed at 39.1 cm^{-1} for the 1:1 complex, while much lower frequency intermolecular vibrations are observed at 8, 15, 34, and 39 cm^{-1} for the 1:2 complex. In the hole-burning spectrum of the 1:2 complex only the intermolecular vibrations are clearly observed. The transitions involving the normal modes of TRN such as 26_0^2, 26_0^4, and 14_0^1 disappeared, suggesting that the normal coordinates of TRN in the S_1 state are significantly changed in the 1:2 complex. A large effect on the normal coordinate changes in the S_1 state by may be due to very floppy nature of TRN in the S_1 state.

3.2. Dispersed fluorescence spectra

Fig. 2 displays the dispersed fluorescence spectra of the origin bands of TRN–$(CO_2)_1$ and TRN–$(CO_2)_2$. Two intermolecular vibrations are observed at 45 and 75 cm^{-1} in the spectrum of the 1:1 complex (upper figure), while four low frequency intermolecular vibrations are observed at 17, 31, 45, and 63 cm^{-1} in the spectrum of the 1:2

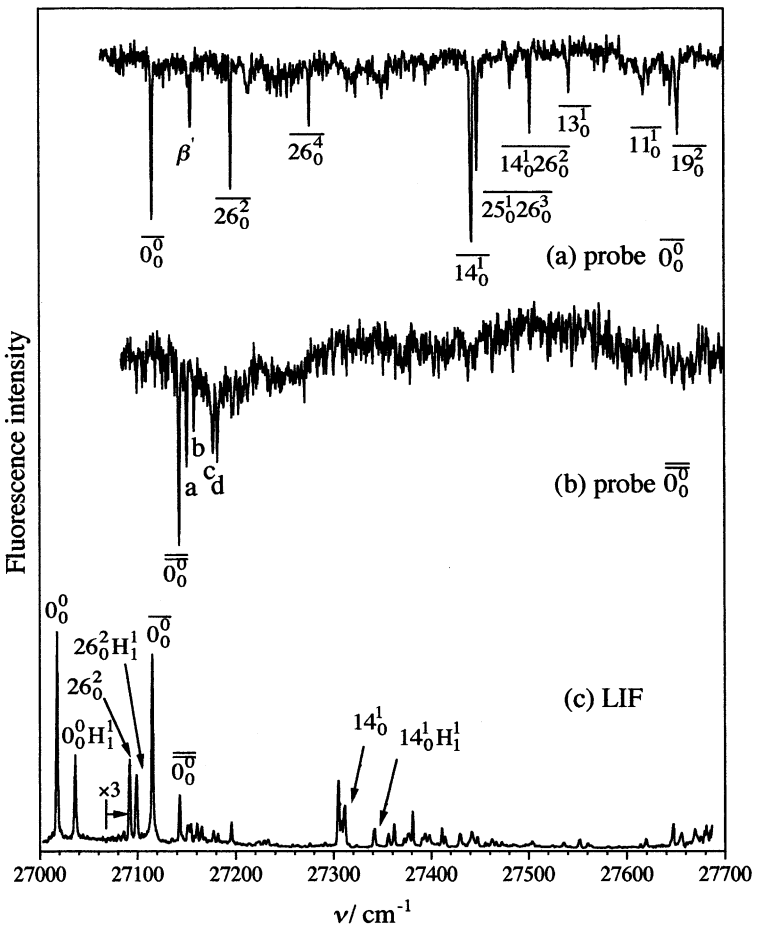

Fig. 1. Hole-burning spectra of (a) TRN–CO_2 and (b) TRN–$(CO_2)_2$ measured by probing the electronic origin bands $\overline{0_0^0}$ and $\overline{\overline{0_0^0}}$ of the 1:1 and 1:2 complexes in the LIF spectrum (c). Four low frequency intermolecular vibrations are indicated by a–d in the spectrum (b). The experimental conditions were $P_0 = 2.5$ atm and $X/D = 40$.

complex (lower figure). The assignments of vibronic bands for the intermolecular vibrational modes of the complexes are provided by comparing the spectra of TRN–$(CO_2)_{1,2}$ with the monomer spectrum. The frequencies of some vibrational levels of TRN–$(CO_2)_1$, 26_2, $25_1 26_1$, 25_2, 14_1, and 11_1 are 8–10 cm^{-1} larger than the corresponding frequencies of the monomer. Similarly, the frequencies of vibronic levels in the S_0 state of the 1:2 complex are somewhat larger than the corresponding frequencies of the monomer. Thus, the normal coordinates in the S_0 state of TRN–$(CO_2)_{1,2}$ changed and the TRN molecule becomes rigid due to the solvation of CO_2. However, the effects of the solvation on the normal coordinate changes in the S_0 state is smaller than those in the S_1 state.

3.3. Structures, binding energies and intermolecular vibrations

The structures of TRN–$(CO_2)_n$ ($n = 1, 2$) are optimized by the DFT calculations at the B3LYP/cc-pVDZ level. The vibrations of TRN–$(CO_2)_n$ ($n = 1, 2$) are calculated by using the same basis set. Three local minima have been obtained for the structure of TRN–$(CO_2)_1$, and are illustrated in Fig. 3. We refer these structures to Isomers I–III. The binding energies for Isomers I–III are 503,

Table 1
Hole-burning spectra of TRN–$(CO_2)_n$ ($n = 1, 2$)

ν/cm^{-1}	$\Delta\nu$/cm^{-1}	Assignment
TRN–$(CO_2)_1$		
27 116	0	0_0^0
27 155	39	Int. (β')[a]
27 197	80	26_0^2
27 277	161	26_0^4
27 443	327	14_0^1
27 448	332	25_0^1 26_0^3
27 503	387	14_0^1 26_0^2
27 543	427	13_0^1
27 646	530	11_0^1
27 653	537	19_0^2
27 756	640	12_0^1
TRN[b]		
27 018	0	0_0^0
27 093	75	26_0^2
27 162	144	26_0^4
27 314	296	14_0^1
27 310	293	25_0^1 26_0^3
27 396	378	14_0^1 26_0^2
27 432	415	13_0^1
27 526	510	11_0^1
27 556	538	19_0^2
27 659	641	12_0^1
TRN–$(CO_2)_2$		
27 144	0	0_0^0
27 152	8	Int.
27 159	15	Int.
27 178	34	Int.
27 183	39	Int.

[a] Intermolecular vibration (see the text and Fig. 4).
[b] The transitions between the (+) tunneling doublet components are listed [5].

390, and 312 cm^{-1}, respectively (Table 2). These values are counterpoise BSSE and zero-point energy (ZPE) corrected energies. The CO_2 molecule binds to the C=O or OH group, providing Isomers I and III, while CO_2 binds to both the C=O and OH groups in Isomer II. Isomer II has essentially the same structure as that reported by MacKenzie et al. [37] who optimized the structure by the HF/6-31G** method, but Isomers I and III have not been reported previously. No local minimum has been obtained for the structure in which CO_2 is located above the molecular plane of TRN.

The calculated frequencies for the intermolecular vibrational modes in the S_0 state are listed in Table 3 together with the observed and calculated vibrational frequencies of the monomer. No significant changes are seen in the calculated vibrational frequencies of the ν_{26}, ν_{25}, ν_{14}, ν_{12}, and ν_{11} modes between the three structures. But the frequencies of intermolecular vibrations clearly depend on the geometry of the complex. The observed vibrational frequencies 45 and 75 cm^{-1} are in good agreement with the calculated frequencies of $\beta'' = 44$ and $\sigma = 73$ cm^{-1} for Isomer I (Fig. 4), and in modest agreement with frequencies $\beta'' = 40$ and $\sigma = 67$ cm^{-1} for Isomer II. The 39 cm^{-1} intermolecular vibration in the S_1 state of the 1:1 complex may correspond to the 45 cm^{-1} vibration (β'') in the S_0 state. The agreement between the calculated and observed frequencies is poor for Isomer III. Thus Isomers I and II are plausible candidates for the observed species, and Isomer I is slightly more favorable than Isomer II from the comparison of the calculated and observed vibrational frequencies.

Three stable structures have been obtained for the 1:2 complex as shown in Fig. 5. These structures are referred to Isomers I–III. Two CO_2 molecules are located at the solvation sites of the 1:1 complex in Isomers I and II, whereas a second CO_2 attaches to Isomer II of TRN–$(CO_2)_1$. The binding energies for Isomers I–III of TRN–$(CO_2)_2$ are 805, 666, and 477 cm^{-1}, respectively. The sum of the binding energies for Isomers I and III of TRN–$(CO_2)_1$ is 815 cm^{-1}. This value is very similar to the binding energy of 805 cm^{-1} for Isomer I of TRN–$(CO_2)_2$, suggesting that interaction between the two CO_2 molecules is very small. The sum of the binding energies for Isomers I and II of TRN–$(CO_2)_1$ is larger than that for Isomer II of TRN–$(CO_2)_2$. In Isomer II of the 1:2 complex two CO_2 molecules strongly interact with the same carbonyl oxygen atom, reducing the binding energy. Thus the difference in the binding energies between Isomers I and II is rather small in the 1:2 complex, but the binding energy for Isomer III is significantly smaller than that for Isomer I. The frequencies of the observed intermolecular vibrations are 17, 31, 45, and 63 cm^{-1}. Several low frequency vibrations are obtained as listed in Table 4 and the combinations of the low frequency vibrations provide similar frequencies very close to the observed ones, preventing from unambiguous

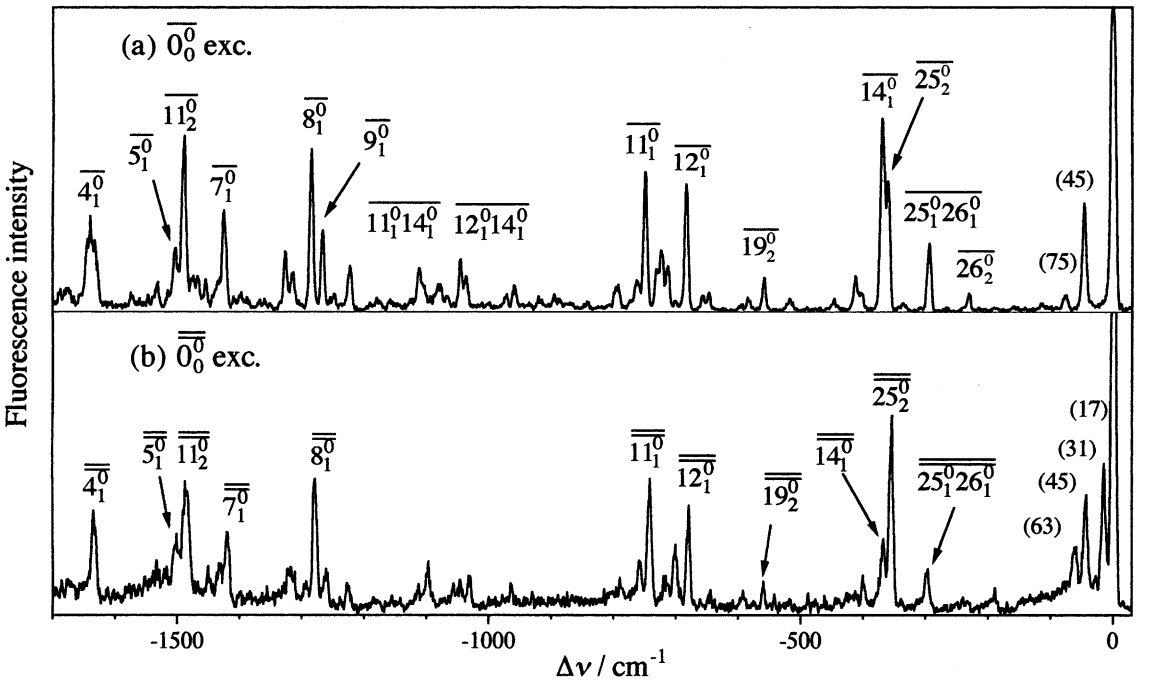

Fig. 2. Dispersed fluorescence spectra of (a) TRN–CO_2 and (b) TRN–$(CO_2)_2$ excited in the electronic origin bands $\overline{0_0^0}$ and $\overline{\overline{0_0^0}}$ of the 1:1 and 1:2 complexes. The values in the parentheses are frequencies for the intermolecular vibrations. The notations for the vibrational modes of TRN are used for the vibrational assignment of the 1:1 and 1:2 complexes.

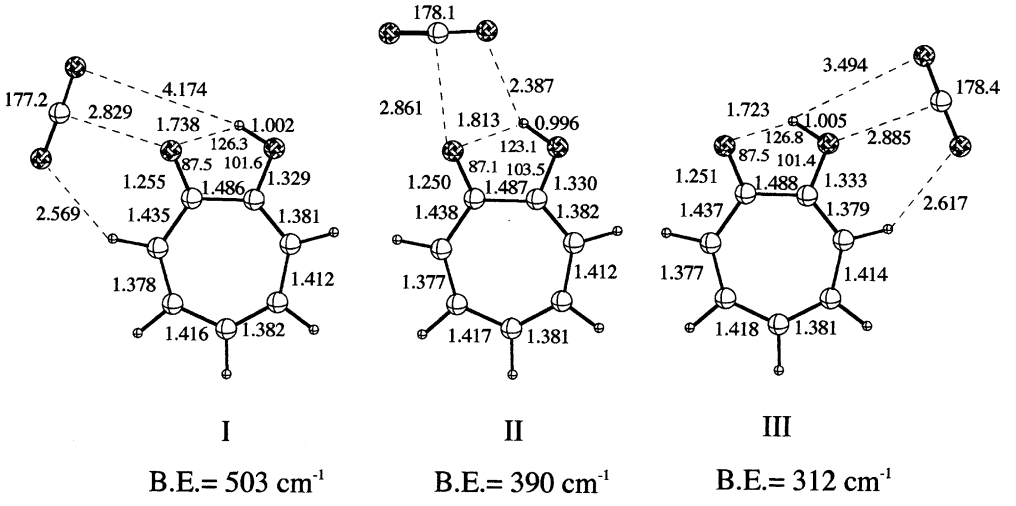

Fig. 3. Optimized structures for TRN–CO_2 1:1 complex obtained by the B3LYP/cc-pVDZ method. The bond distances (Å) and bond angles (°) around the C=O···O–H moiety are indicated in the figure.

assignment of the observed species. The observed species is likely to be either Isomer I or II from the comparison of the calculated binding energies.

The atomic point charges have been calculated based upon Mulliken population analysis. The CO_2 molecule has a large quadrupole moment and

Table 2
Calculated binding energies (cm^{-1}) for TRN–$(CO_2)_n$ ($n = 1, 2$)

	BE[a]	BSSE	BE (BSSE corrected)[b]
TRN–$(CO_2)_1$			
Isomer I	1306	803	503
Isomer II	1017	705	312
Isomer III	1044	654	390
TRN–$(CO_2)_2$			
Isomer I	2309	1504	805
Isomer II	2010	1345	666
Isomer III	1515	1038	477

[a] ZPE corrected binding energy.
[b] ZPE and BSSE energy corrected binding energy.

a large positive charge is centered on the carbon atom of CO_2, while the two oxygen atoms are negatively charged. The oxygen atoms of the C=O and OH groups of TRN are negatively charged, providing a large local dipole moment in the C=O or OH group. Thus, in a classical picture the dipole–quadrupole interaction between CO_2 and C=O/OH is major intermolecular interaction in the complex. It is evident that the hydrogen bonding interaction is insignificant in Isomers I and III since the distance between the hydroxy proton and the oxygen atom of CO_2 is long (4.174 and 3.494 Å). However, the distance between the hydroxy proton and an oxygen atom of CO_2 (2.387 Å) is much shorter in Isomer II than those in the other two structures. Therefore, the hydrogen bonding interaction may contribute to stabilize in Isomer II in addition to the electrostatic interaction between the C=O group and CO_2.

3.4. Quench of proton tunneling

The TRN–CO_2 complexes have unique features as compared with the nonplanar TRN–M vdW complexes and the hydrogen-bonded complexes of TRN with polar molecules studied so far. In TRN–$(CO_2)_1$ the CO_2 molecule is located in the molecular plane of TRN, therefore, the nature of intermolecular interaction is different from the other TRN–M complexes. The present work suggested that either Isomer I or II of TRN–$(CO_2)_1$ may correspond to the observed species, and Isomer I is slightly more favorable than Isomer II. Isomers I and III correspond to the structure of two minima in the double-minimum potential well along the tunneling coordinate. The calculated energy difference between the two minima is 192 cm^{-1}, suggesting that the double-minimum potential well along the proton transfer coordinate is highly asymmetric. It is predicted that the proton tunneling will be completely quenched if the energy difference of the two minima ΔE is larger than the tunneling splitting [39]. The tunneling splitting in the zero-point level of the S_1 state is 19 cm^{-1} [2–5]. Therefore, the asymmetry in the double-minimum potential well is large enough to quench the tunneling splitting. No local minimum has been

Table 3
Calculated vibrational frequencies (cm^{-1}) for the S_0 state of TRN–$(CO_2)_1$

TRN–$(CO_2)_1$					TRN	
Calculated[a]				Experimental	Calculated[a]	Experimental
Mode	Isomer I	Isomer II	Isomer III			
β	20	14	10			
γ	28	29	32			
β'	44	40	36	45		
σ	73	67	61	75		
γ'	104	90	103			
26	125	124	120	116	123	109
25	183	185	184	178	181	178
14	369	370	364	369	363	360
12	687	686	688	681	679	674
11	738	739	741	747	732	741

[a] $f = 0.983$ is used as a scaling factor.

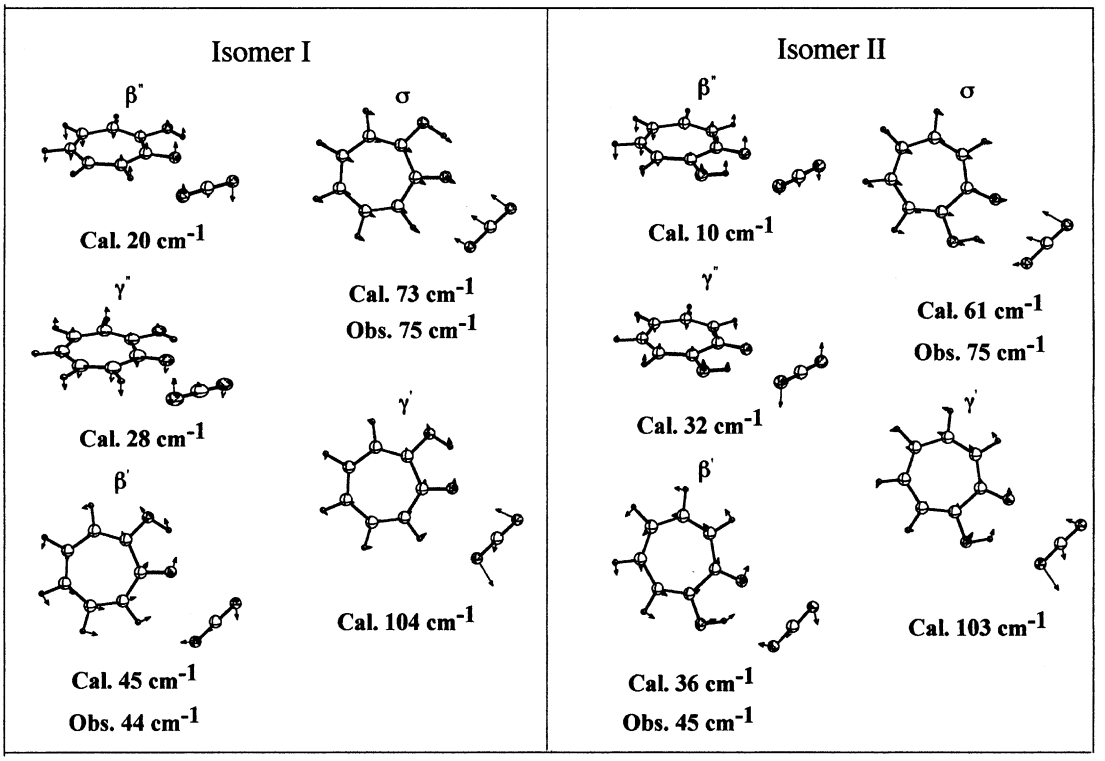

Fig. 4. Calculated low frequency intermolecular modes for structure I and II of TRN–CO_2. The displacements of the atoms are indicated by the arrows.

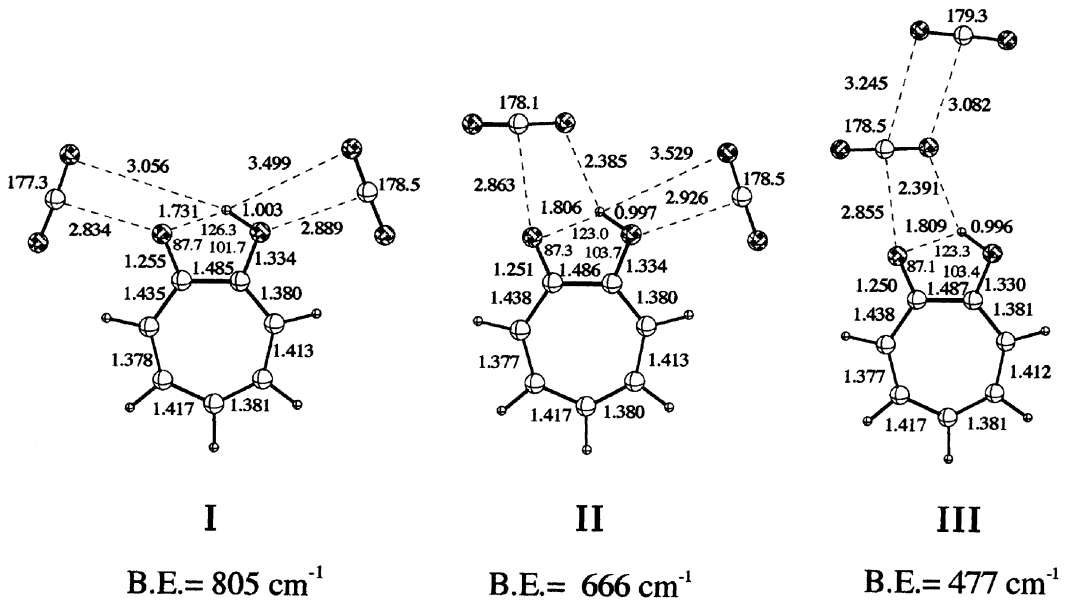

Fig. 5. Optimized structures for TRN–CO_2 1:2 complex obtained by the B3LYP/cc-pVDZ method. The bond distances (Å) and bond angles (°) around the C=O···O–H moiety are indicated in the figure.

Table 4
Vibrational frequencies (cm^{-1}) for intermolecular modes of TRN–$(CO_2)_2$

Isomer I	Isomer II	Isomer III
Calculated (S_0)[a]		
15	7	7
19	15	10
26	21	14
26	30	21
34	32	33
51	47	37
65	58	40
72	66	61
90	87	71
105	107	130
Experimental		
S_0		S_1
17		8
31		15
45		34
63		39

[a] $f = 0.983$ is used as a scaling factor.

obtained for proton transferred structure when Isomer II was assumed to be the most stable structure, therefore, proton transfer must be inhibited in Isomer II.

The binding energy is 503 cm^{-1} for Isomer I of the 1:1 complex. The binding energy previously reported is 1070 cm^{-1}, which is calculated at the HF/6-31G** level without BSSE correction [37]. The binding energy for TRN–$(CO_2)_1$ obtained in the present work (503 cm^{-1}) is about a half that (1070 cm^{-1}) at the HF/6-31G** level [37], and much smaller than for the exterior structure of TRN–$(H_2O)_1$ calculated at the B3LYP/6-31+G′[2d,p]w (1512 cm^{-1}) and MP2/6-31+G′[2d,p]w level (1746 cm^{-1}) levels [25]. The calculated binding energies for Isomers I–III of the 1:2 complex are 805, 666, and 477 cm^{-1}, respectively. The largest binding energy 805 cm^{-1} is much smaller than that for TRN–$(H_2O)_1$. The calculated value is consistent with the smaller spectral blue shift of the 0–0 transition energy for the TRN–$(CO_2)_2$ than that for TRN–$(H_2O)_1$. If the most stable structure is Isomer I, the double-minimum potential well along the tunneling coordinate is symmetric. However, two C_S structures may be significantly stabilized due to the attachment of CO_2 close to the C=O group as compared with the C_{2v} structure, and the effective tunneling potential energy barrier may increase. In Isomers II and III the tunneling potential must be highly asymmetric. In addition, the calculations suggest that the hydrogen-bond distance is increased. Thus, the non-observation of proton tunneling is consistent with the theoretical results.

3.5. Comparison with other complexes

The observed blue-shifts of the S_1–S_0 transition energies for TRN–$(CO_2)_n$ ($n = 1, 2$) provide insights into intermolecular interaction in the complexes. We ascribed a large blue-shift of the S_1–S_0 transitions energy in the excitation spectrum of TRN–$(CH_3COCH_3)_1$ complex [28] to weakening of the intramolecular hydrogen bond in TRN that raises the energy in the S_1 state. Similar blue-shifts have been observed in various hydrogen-bonded complexes of TRN, and the magnitude of the blue-shift is nearly proportional to the binding energy of the hydrogen-bonded complex [37]. The geometries of Isomers I and II of TRN–$(CO_2)_1$ are very similar to the exterior and ring structures of TRN–$(H_2O)_1$ [24–26]. The blue-shifts of the transition energy of TRN–$(CO_2)_1$ is 98 cm^{-1}, while that of TRN–$(H_2O)_1$ is 289.0 cm^{-1} [24]. The blue-shift of TRN–$(CO_2)_1$ is a third that of TRN–$(H_2O)_1$. The calculated binding energy for TRN–$(CO_2)_1$ (1.76 kcal/mol) is about a quarter of the binding energy for TRN–$(H_2O)_1$ (4.32 kcal/mol) [25]. The observed small blue-shift of TRN–$(CO_2)_1$ is consistent with a small binding energy.

The structure and intermolecular interaction in TRN–$(CO_2)_1$ could be compared with those of the TRN–$(N_2)_1$ and TRN–$(CO)_1$ complexes [33]. In TRN–N_2,CO the electronic origins are red-shifted relative to the origin of the monomer and the hole-burning spectrum indicates that only one species is observed. We concluded that the solvent molecule is located above the seven-membered ring [33], although Sinha et al. [35] proposed the observation of a planer TRN–$(CO)_1$ in addition to the nonplanar complex. The electric quadrupole moments of N_2, CO, and CO_2 are -5.07×10^{-40}, -6.51×10^{-40}, and -14.4×10^{-40} $C\,m^2$ [39], respectively. The dipole–quadrupole interaction between

TRN and N_2/CO must be smaller than that between TRN and CO_2, and the dispersive interaction must be dominant in the TRN–N_2,CO complexes.

The character of the intermolecular interaction in TRN–$(CO_2)_1$ becomes clear by comparing its structure with those of the CO_2–H_2O [40,41] and phenol–N_2,CO [42–46] 1:1 complexes. The microwave spectrum of CO_2–H_2O showed that the most stable structure of CO_2–H_2O is T-shaped [40,41]. A large positive charge on the carbon atom of CO_2 strongly interacts with the dipole moment of H_2O, stabilizing the T-shaped structure. Very similar interaction may exist in Isomers I and III of TRN–$(CO_2)_1$. The intermolecular interaction in Isomer II seems to be complicated due to the interaction between the hydroxy proton and the oxygen atom of CO_2, but the origin of the interaction must be the same as that in Isomers I and III.

Recently, Haines et al. measured the resonance enhanced mutiphoton ionization and zero electron kinetic energy spectra of the phenol–N_2, CO 1:1 complexes [42–46]. On the basis of the experimentally determined binding energies for the complexes it was suggested that in the phenol–N_2 complex the N atom is bonded to the H atom of the OH group, while the C atom is bonded with the H atom of the OH group in phenol–$(CO)_1$ [43,44]. The structure of phenol–N_2 was supported by the measurement of the OH stretching frequency [46] and also by ab initio calculations [45]. It was concluded that the N_2 or CO molecule is nearly linearly bonded to the hydroxy proton of phenol, and the intermolecular hydrogen bond is formed in phenol–N_2,CO. The intermolecular interaction in these complexes is originating from the interaction of the quadrupole moment of N_2 or CO with the dipole moment of the OH group [42–45]. Thus, two types of intermolecular interaction observed in H_2O–CO_2 and phenol–N_2,CO may simultaneously exist in Isomer II of TRN–$(CO_2)_1$.

4. Conclusion

The structure of the TRN–$(CO_2)_n$ $(n = 1, 2)$ complexes and the effects of solvation on proton tunneling in TRN have been re-investigated by combining the measurement of the hole-burning and dispersed fluorescence spectra with the DFT. The vibronic transitions of the 1:1 and 1:2 complexes have been well separated, allowing us to assign vibronic bands in the S_1 state. The calculations at the B3LYP/cc-pVDZ level suggested that TRN has three solvation sites in the molecular plane, providing three isomers for the 1:1 complexes. These three isomers are stabilized by electrostatic interaction mainly due to the quadrupole moment of CO_2 and the dipole moment of the C═O and OH groups of TRN. Isomers I and II are candidates for the observed species. The intermolecular vibrational frequencies as well as the binding energies are similar one another in the two isomers, preventing from unambiguous assignment of the observed species. The calculations suggest that the double-minimum potential well along the tunneling coordinate is asymmetric for the 1:1 complex, in consistent with the inhibition of proton tunneling even for the excitation of the tunneling promoting mode ν_{13} or ν_{14} of TRN. Similarly, the calculations suggested the existence of three isomers for the 1:2 complex. The normal coordinates of TRN in the 1:2 complex remarkably change in the S_1 state.

Acknowledgements

This work was partly supported by a Grant-in-Aid for Scientific Research no. 11440177 from the Ministry of Education, Science, Sports and Culture of Japan.

References

[1] Y. Tomioka, M. Ito, N. Mikami, J. Phys. Chem. 87 (1983) 4401.
[2] A.C.P. Alves, J.M. Hollas, H. Musa, T. Ridley, J. Mol. Spectrosc. 109 (1985) 99.
[3] R.L. Redington, Y. Chen, G.J. Scherer, R.W. Field, J. Chem. Phys. 88 (1988) 627.
[4] R.L. Redington, T.E. Redington, H. Hunter, R.W. Field, J. Chem. Phys. 92 (1990) 6447.
[5] H. Sekiya, Y. Nagashima, Y. Nishimura, J. Chem. Phys. 92 (1990) 5761.
[6] H. Sekiya, Y. Nagashima, Y. Nishimura, Chem. Phys. Lett. 160 (1989) 581.

[7] H. Sekiya, K. Sasaki, Y. Nishimura, Z.-H. Li, A. Mori, H. Takeshita, Chem. Phys. Lett. 173 (1990) 285.
[8] H. Sekiya, Y. Nagashima, T. Tsuji, Y. Nishimura, A. Mori, H. Takeshita, J. Phys. Chem. 95 (1991) 10311.
[9] T. Tsuji, H. Sekiya, Y. Nishimura, R. Mori, A. Mori, H. Takeshita, J. Chem. Phys. 97 (1992) 6032.
[10] R.K. Frost, F.C. Hagemeister, C.A. Arrington, T.S. Zwier, K.D. Jordan, J. Chem. Phys. 105 (1996) 2595.
[11] K. Nishi, H. Sekiya, H. Kawakami, A. Mori, Y. Nishimura, J. Chem. Phys. 109 (1998) 1589.
[12] K. Nishi, H. Sekiya, H. Kawakami, A. Mori, Y. Nishimura, J. Chem. Phys. 111 (1999) 3961.
[13] K. Tanaka, H. Honjo, T. Tanaka, H. Kouguchi, Y. Ohshima, Y. Endo, J. Chem. Phys. 110 (1999) 1969.
[14] R.L Redington, T.E. Redington, J.M. Montgometry, J. Chem. Phys. 113 (2000) 2304.
[15] R.L. Redington, C.W. Bock, J. Phys. Chem. 95 (1991) 10284.
[16] M.V. Vener, S. Scheiner, N.D. Sokolov, J. Chem. Phys. 101 (1994) 9755.
[17] N. Sanna, F. Ramondo, L.J. Bencivenni, J. Mol. Struct. 318 (1994) 217.
[18] S. Takada, H. Nakamura, J. Chem. Phys. 102 (1995) 3977.
[19] J.J. Paz, M. Moreno, J. Lluck, J. Chem. Phys. 103 (1995) 353.
[20] Z. Smedarchina, W. Siebrand, M.Z. Zgierski, J. Chem. Phys. 104 (1996) 1203.
[21] M.J. Wojcik, H. Nakamura, S. Iwata, W. Tatara, J. Chem. Phys. 112 (2000) 6322.
[22] R. Rossetti, L.E. Brus, J. Chem. Phys. 73 (1980) 1546.
[23] T. Ikoma, K. Akiyama, S. Tero-Kubota, Y. Ikegami, J. Chem. Phys. 111 (1999) 6875.
[24] H. Sekiya, H. Hamabe, H. Ujita, N. Nakano, Y. Nishimura, Chem. Phys. Lett. 255 (1996) 437.
[25] R.K. Frost, F.C. Hagemeister, C.A. Arrington, D. Schleppenbach, T.S. Zwier, K.D. Jordan, J. Chem. Phys. 105 (1996) 2605.
[26] A. Mitsuzuka, A. Fujii, T. Ebata, N. Mikami, J. Chem. Phys. 105 (1996) 2618.
[27] O. Mo, M. Yanez, J. Phys. Chem. 102 (1998) 8174.
[28] H. Hamabe, H. Sekiya, N. Nakano, K. Nishi, Y. Nishimura, Chem. Phys. Lett. 280 (1997) 390.
[29] H. Sekiya, T. Nakajima, H. Ujita, T. Tsuji, S. Ito, Y. Nishimura, Chem. Phys. Lett. 215 (1993) 499.
[30] H. Sekiya, H. Hamabe, T. Nakajima, A. Mori, H. Takeshita, Y. Nishimura, Chem. Phys. Lett. 224 (1994) 563.
[31] H. Sekiya, H. Hamabe, H. Ujita, N. Nakano, Y. Nishimura, J. Chem. Phys. 103 (1995) 3895.
[32] H. Sekiya, H. Hamabe, H. Ujita, N. Nakano, Y. Nishimura, Chem. Phys. Lett. 255 (1996) 437.
[33] H. Hamabe, T. Fukuchi, S. Shiraishi, K. Nishi, Y. Nishimura, T. Tsuji, N. Nishi, J. Phys. Chem. 102 (1998) 3880.
[34] H.K. Sinha, R.P. Steer, Chem. Phys. Lett. 241 (1995) 328.
[35] H.K. Sinha, V.J. MacKenzie, R.P. Steer, Chem. Phys. 213 (1996) 397.
[36] V.J. MacKenzie, R.P. Steer, Res. Chem. Intermed. 24 (1998) 803.
[37] V.J. MacKenzie, M.Z. Zgierski, R.P. Steer, J. Phys. Chem. 103 (1999) 8389.
[38] M.J. Frisch, G.W. Trucks, H.B. Schlegel, G.E. Scuseria, M.A. Robb, J.R. Cheeseman, V.G. Zakrzewski, J.A. Montgomery Jr., R.E. Stratmann, J.C. Burant, S. Dapprich, J.M. Millam, A.D. Daniels, K.N. Kudin, M.C. Strain, O. Farkas, J. Tomasi, V. Barone, M. Cossi, R. Cammi, B. Mennucci, C. Pomelli, C. Adamo, S. Clifford, J. Ochterski, G.A. Petersson, P.Y. Ayala, Q. Cui, K. Morokuma, D.K. Malick, A.D. Rabuck, K. Raghavachari, J.B. Foresman, J. Cioslowski, J.V. Ortis, A.G. Baboul, B.B. Stefanov, G. Liu, A. Liashenko, P. Piskorz, I. Komaromi, R. Gomperts, R.L. Martin, D.J. Fox, T. Keith, M.A. Al-Laham, C.Y. Peng, A. Nanayakkara, C. Gonzalez, M. Challacombe, P.M.W. Gill, B. Johnson, W. Chen, M.W. Wong, J.L. Andres, C. Gonzalez, M. Head-Gordon, E.S. Replogle, J.A. Pople, GAUSSIAN 98, revision A.7, Gaussian Inc., Pittsburgh, PA, 1998.
[39] R. Rossetti, R. Rayford, R.C. Haddon, L.E. Brus, J. Am. Chem. Soc. 103 (1981) 4303.
[40] S.C. Khristenko, A.I. Maslov, V.P. Shevelko, Molecules and their Spectroscopic Properties, Springer, Berlin, 1997, p. 81.
[41] K.I. Peterson, W. Klemperer, J. Chem. Phys. 80 (1984) 2439.
[42] G. Columberg, A. Bauder, N. Heineking, W. Stahl, J. Makarewiz, Mol. Phys. 93 (1998) 215 and references therein.
[43] S.R. Haines, W.D. Geppert, D.M. Chapman, M.J. Watkins, C.E.H. Dessent, M.C.R. Cockett, K. Muller-Dethlefs, J. Chem. Phys. 109 (1998) 9244.
[44] S.R. Haines, C.E.H. Dessent, K. Müller-Dethlefs, J. Chem. Phys. 111 (1999) 1947.
[45] D.M. Chapman, K. Müller-Dethlefs, B. Peer, J. Chem. Phys. 111 (1999) 1955.
[46] A. Fujii, M. Miyazaki, T. Ebata, N. Mikami, J. Chem. Phys. 110 (1999) 11125.